

Competition and coexistence of bond and charge orders in $(\text{TMTTF})_2\text{AsF}_6$

F. Zamborszky^{1,2}, W. Yu¹, W. Raas¹, S. E. Brown¹, B. Alavi¹, C. A. Merlic³, A. Baur³

¹ *Department of Physics and Astronomy, UCLA, Los Angeles, California 90095-1547*

² *Los Alamos National Laboratory, Los Alamos, New Mexico 87545 and*

³ *Department of Chemistry and Biochemistry, UCLA, Los Angeles, California 90095-1569*

(Dated: October 23, 2018)

$(\text{TMTTF})_2\text{AsF}_6$ undergoes two phase transitions upon cooling from 300 K. At $T_{CO}=103$ K a charge-ordering (CO) occurs, and at $T_{SP}(B=9\text{ T})=11$ K the material undergoes a spin-Peierls (SP) transition. Within the intermediate, CO phase, the charge disproportionation ratio is found to be at least 3:1 from ^{13}C NMR T_1^{-1} measurements on spin-labeled samples. Above T_{SP} up to about $3T_{SP}$ T_1^{-1} is independent of temperature, indicative of low-dimensional magnetic correlations. With the application of about 0.15 GPa pressure, T_{SP} increases substantially, while T_{CO} is rapidly suppressed, demonstrating that the two orders are competing. The experiments are compared to results obtained from calculations on the 1D extended Peierls-Hubbard model.

PACS numbers: 71.20.Rv, 71.30.+h, 71.45.Lr, 76.60.-k

Inhomogenous charge and spin structures are a consequence of competing interactions and therefore of general interest in correlated electron systems. Examples include the high- T_c cuprates¹ and manganites² as well as the quasi-2D organic conductors³. The quasi-1D salts made from TMTTF or TMTSF molecules are also susceptible to charge-ordered states. Independent of that, they are well-known for the sequence of ground states accessible by applying pressure or selecting different counterions. For example, the material $(\text{TMTTF})_2\text{PF}_6$ undergoes transitions from spin-Peierls, antiferromagnetic (AF), spin-density wave (SDW), and finally to superconducting (SC) ground states as the pressure is increased to 4-5 GPa^{4,5}. For a long time, it was known that another phase transition occurs in a number of TMTTF salts with both centrosymmetric (*e.g.*, AsF_6 , SbF_6) and non-centrosymmetric (*e.g.*, ReO_4) counterions. Only recently^{6,7} was the broken symmetry associated with this transition identified as a charge disproportionation.

In TMTTF salts the characteristic temperature of the onset of the charge-ordered (CO) phase is high, on the order of 100 K. It indicates that the interactions driving the CO are relatively strong, and therefore potentially impact the electronic and magnetic properties of the disordered phase. Issues associated with CO correlations in these systems take particular relevance when considering that the nature of the metallic phase of TMTSF salts remains controversial^{8,9,10}. Below we report the results of a number of NMR measurements on ^{13}C spin-labeled samples of $(\text{TMTTF})_2\text{AsF}_6$ in the CO phase. Our principle result is a mapping of the temperature/pressure phase diagram of the SP and CO phases that includes a tetracritical point with a region of coexistence of the two forms of order. There is good agreement between the experiments and the results of calculations on the 1D extended Hubbard¹¹ and Peierls-Hubbard models^{12,13}.

A review of the characteristics of the CO phase and the phase transition is in order. With counterions PF_6 , AsF_6 , and SbF_6 , the ordering temperature is 62 K, 103 K, and 154 K, respectively. Upon cooling, the salts made with

the first two are already well into a region of thermally activated resistivities when the CO transition occurs. The last one undergoes a continuous metal/semiconductor transition at T_{CO} . The mystery of the order parameter arose from the fact that no evidence for a superlattice was ever found with X-ray scattering. Charge order was identified as the proper description of the order parameter from NMR studies⁷. At high temperatures, the unit cell consists of two equivalent TMTTF molecules related by inversion about the counterion¹⁴. A low-frequency divergence of the real part of the dielectric susceptibility χ_e is consistent with mean-field-like ferroelectric behavior^{6,15}. The observations were taken as evidence for a breaking of the inversion symmetry within the unit cell, and the spontaneous dipole moment is associated with the charge imbalance on the two molecules.

All of the experiments were performed in $B_0 = 9$ T magnetic field (^{13}C NMR frequency $\nu=96.4$ MHz). Pressure was applied using a self-clamping BeCu cell, with Flourinert 75 serving as the pressure medium. The reproducible low-temperature pressure was calibrated in separate runs by measuring inductively the change of the superconducting transition temperature of lead. The NMR coil was constructed so that the molecular stacking axis (\mathbf{a}) was oriented normal to the static magnetic field. Any significant reorientation about \mathbf{a} between experimental runs is excluded by noting that the ^{13}C inter-nuclear dipolar coupling remained unchanged.

In Fig. 1 we show the temperature dependence of the relative hyperfine shifts for all of the unique ^{13}C sites. Once the molecules are inside the solid, the two sites forming the bridge are inequivalent and have different hyperfine shifts. At high temperatures the two molecules within the unit cell are equivalent. Below the phase transition at $T_{CO}=103$ K, each of the two lines split into two peaks with equal absorption strengths. We showed this to be a result of a charge disproportionation developing between two inequivalent molecules, and the order parameter amplitude is proportional to the difference of the NMR frequencies within each of the split lines. The

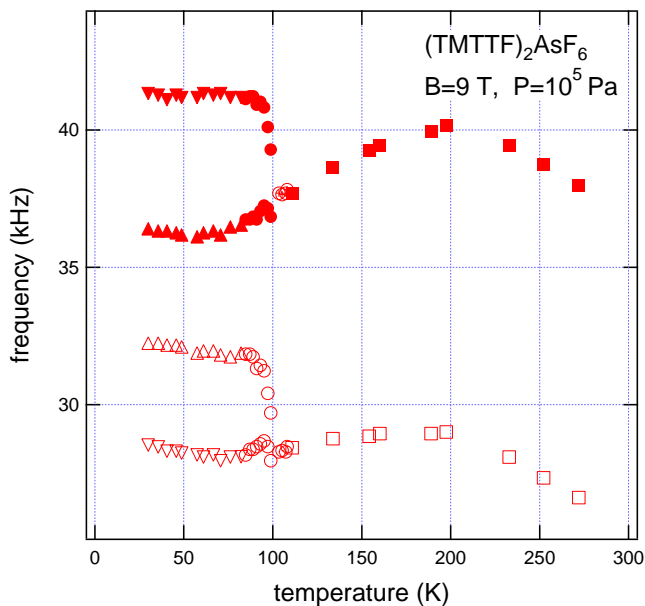


FIG. 1: Positions of the ^{13}C NMR peaks versus temperature at the magic angle at ambient pressure for $(\text{TMTTF})_2\text{AsF}_6$. The CO transition takes place at $T_{\text{CO}}=103$ K.

character of the transition is 2nd order.

The amplitude of the charge disproportionation can be estimated from the spin lattice relaxation rates. These are shown in Fig. 2. The relaxation rates are about one order of magnitude faster on one of the two types of molecules. Ideally, we expect that T_1^{-1} , dominated by hyperfine coupling, is proportional to the electronic density on a particular molecule. For isotropic hyperfine interaction and no spectral overlap whatsoever between the respective absorption lines, $T_1^{-1} \propto \rho^2$, with ρ the molecular charge count. Neither one of these conditions is strictly true here, so the ratio of the relaxation rates of sites on the high- and low-density molecules determines a *lower bound* for the disproportionation, namely 3:1.

Modest applied pressures strongly depress T_{CO} . The order parameter of the CO phase, taken from the temperature dependence of the splitting of the NMR lines, is shown in Fig. 3 at different pressures. Three effects are visible as the pressure is increased: 1) The maximum splitting is decreased. 2) T_{CO} is decreased. 3) The order parameter develops much less steeply.

T_{SP} is identified from the temperature dependence of either ^{13}C or ^{75}As T_1^{-1} . ^{13}C is a spin $I=1/2$ nucleus for which T_1^{-1} falls precipitously below T_{SP} . ^{75}As , on the other hand, has spin $I=3/2$, so it couples to electric field gradient (EFG) fluctuations produced, for example, by lattice vibrations. The peak in ^{75}As T_1^{-1} at T_{SP} is naturally associated with the critical slowing down of the soft $2k_{\text{F}}$ phonons¹⁶. The completed phase diagram for $(\text{TMTTF})_2\text{AsF}_6$ appears in Fig. 4. The CO phase diminishes quite rapidly: $P = P_c \lesssim 0.15$ GPa is enough to suppress it.

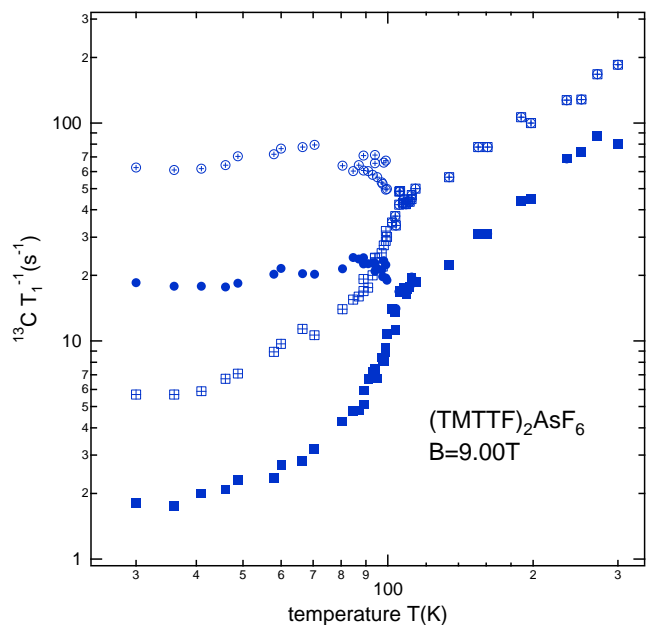


FIG. 2: $^{13}\text{C} T_1^{-1}$ relaxation rate as a function of temperature at ambient pressure in $(\text{TMTTF})_2\text{AsF}_6$. Spectra were taken at the magic angle, the magnetization recovery was obtained by integrating over the distinct peaks of the absorption spectra. Similar markers represent $^{13}\text{C} T_1^{-1}$ of peaks evolving from the same high temperature peak.

The phase diagram has a remarkable feature: while T_{CO} is decreasing, T_{SP} increases significantly up to about 150% of its ambient pressure value. After the CO is suppressed at P_c , T_{SP} decreases weakly with additional pressure. The maximum of T_{SP} at P_c indicates that the CO site order and the SP bond order are competing. If the competition is sufficiently weak, the order parameters will coexist. Otherwise, a first-order transition line divides the two phases. In principle, the CO and SP order parameters could be simultaneously characterized by X-ray scattering experiments. To date, we are not aware of a published X-ray report of the CO phase, even at ambient pressure. We call attention to this not only because NMR is a local probe, but also because the methods described above for determining the CO order parameter do not work in the SP phase. This is because the paramagnetic shifts are nearly absent for the singlet ground state and all ^{13}C sites are equivalent. There is an exception: magnetic fields B larger than a critical value B_c produce an incommensurate (I) phase, through the generation of triplet excitations. In a 1D picture, the triplets consist of soliton/anti-soliton pairs. Typically $B_c \propto T_{\text{SP}}$. Although it is not measured for $(\text{TMTTF})_2\text{AsF}_6$, we know that $B_c=19$ T for the PF_6 salt¹⁷. Applied fields greater than 19 T resulted in broadened NMR lines associated with the staggered spin density of the excitations¹⁸. Lineshapes demonstrating the effect near to B_c are shown in Fig. 5. At low fields, we see a single line showing that all ^{13}C sites are equivalent in the SP phase. If the CO is still

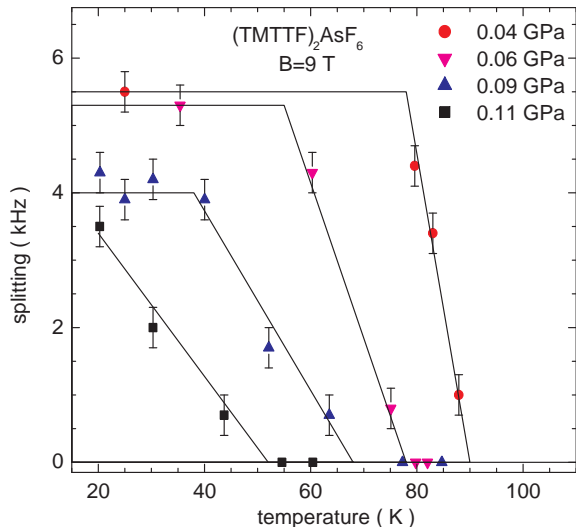


FIG. 3: The order parameter as a function of temperature at various pressures. The solid lines are guide to the eye.

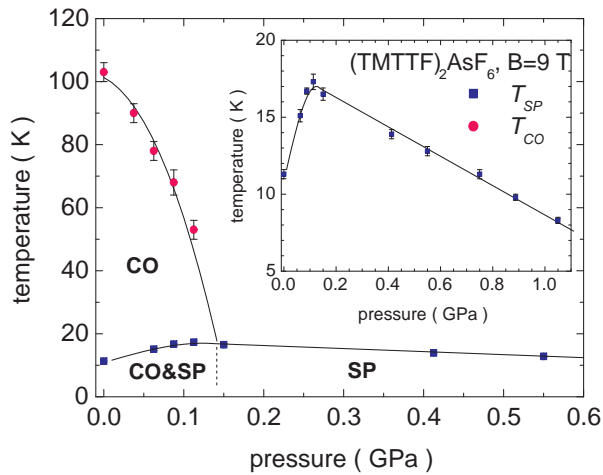


FIG. 4: Phase diagram of $(\text{TMTTF})_2\text{AsF}_6$ established from NMR experiments at $B=9$ T. The lines are a guide to the eye. The dashed line is used only to emphasize that a region of coexistence is present.

present, we expect the absorption at high fields to consist of exactly 4 contributions all of which are identical. Two contributions are expected without the CO. Four *well-separated* "ledges" are evident on each side of the maximum at the higher field, which we interpret as coming from the nuclei near the center of the soliton-like excitations where the staggered spin density is maximum^{19,20}. The substantial differences in hyperfine fields on the four

sites indicates that the disproportionation remains large even in the ground state, *i.e.*, the two orders coexist as shown in Fig. 4. A smaller charge disproportionation is also expected in the SP phase¹³ at high pressures, but our experimental setup did not allow to investigate it.

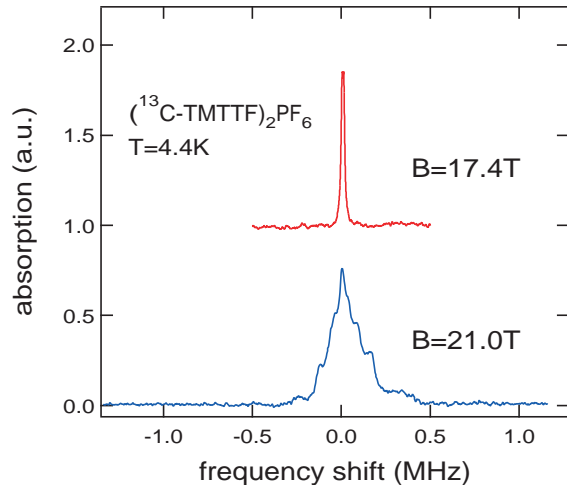


FIG. 5: ^{13}C NMR lineshapes of $(\text{TMTTF})_2\text{PF}_6$ at fields close to the critical field B_c , at ambient pressure. The broadening for $B > B_c$ is characteristic of the incommensurate phase.

We should emphasize that the 1D extended Peierls-Hubbard model contains most of the essential physics that produces the observed phase diagram. Justification for a quasi-1D point of view follows from the fact that the molecular spacing along the stack alternates¹⁴. It can be modeled by introducing intrachain hopping integrals t_1 and t_2 along the stack. Therefore, the system is half-filled and electron-electron Umklapp scattering in 1D opens a charge gap Δ_p ²¹. Provided that $\Delta_p \gg t_\perp$, where t_\perp is the transverse hopping, 1D confinement leads to an insulating state even at high temperatures and at $T > T_{CO}$.

Without phonon coupling, the 1D extended Hubbard model will produce a CO state if the Coulomb interaction is sufficiently large and long-ranged²¹, *i.e.*, the nearest-neighbor interaction $V > V_c$ ¹¹. In the TMTTF salts, it is expected that V is very close to the predicted threshold obtained in strong-coupling perturbation theory^{13,22}. Further, the large lower bound that we infer for the charge disproportionation is quantitatively reasonable when compared to model parameters^{11,13}. The principle effect of pressure is to increase the hopping integrals, which leads to a rapid destabilization of the CO phase, just as we observe. $P > P_c$ results in a SP ground state, once the phonon coupling is included.

Regarding the high-temperature CO phase, there are two qualitative differences between recent numerical works and our experimental observations. One of them is the expectation that the CO occurs together with the metal-insulator transition¹³. The other is the character of the transition. The measurements are consistent with

the CO phase transition being a continuous one along the entire line, whereas *mean-field* calculations describe the transition as first order. Including the dimerization of the 1D stack is known to eliminate the first-order character in the mean-field calculations of the 1D extended Hubbard model¹¹. Therefore, it is very likely that the dimerization is crucial in *three* respects. First, it confines coherent charge motion to the stacks and because of this it is appropriate to compare to 1D models. Second, the confinement assures that a metal-insulator crossover occurs at a high temperature, perhaps far above T_{CO} . Third, it changes the character of the CO transition from first-order to second-order.

Returning to the issue of metal vs. insulator in the TMTTF salts, there is one choice of centrosymmetric counterion, SbF_6 , which undergoes a real transition to an insulating state at T_{CO} ²³. The reason is thought to be that the larger size of SbF_6 relative to, say PF_6 , leads to a smaller difference between the alternating hopping integrals, t_1 and t_2 , and the 1D Umklapp scattering is not strong enough relative to t_\perp to open the charge gap. It still undergoes a CO transition at $T_{CO}=154$ K, though the system should be thought of as inherently

quasi-2D. Consequently, we do not expect the ground state to have spin-Peierls character, and indeed, it is antiferromagnetic²⁴.

In conclusion, we studied the pressure dependence of the relative stability of the CO and SP phases observed in $(\text{TMTTF})_2\text{AsF}_6$ using ^{13}C NMR spectroscopy and spin-lattice relaxation measurements. The coexistence of the two orders was established along with the existence of a tetracritical point in the temperature/pressure phase diagram. The CO phase is suppressed easily with modest pressure; the natural interpretation is that it results from the effect of the increasing bandwidth relative to the strength of the near neighbor Coulomb repulsion V within the stacks. The lower-bound for the charge disproportionation is set at 3:1. The phase diagram and disproportionation amplitude are consistently compared to results of calculations on the 1D extended Hubbard and Peierls-Hubbard models.

ACKNOWLEDGEMENTS. The work was supported by the NSF under grant no. DMR-9971530. We would like to acknowledge helpful discussions with S. Brazovskii, R. T. Clay, S. Kivelson, and S. Mazumdar.

-
- ¹ J. M. Tranquada, B. J. Sternlieb, J. D. Axe, Y. Nakamura, and S. Uchida, *Nature* **375**, 561 (1995).
- ² S. Mori, C. H. Chen, and S. W. Cheong, *Nature* **392**, 473 (1998).
- ³ K. Miyagawa, A. Kawamoto, and K. Kanoda, *Phys. Rev. B* **62**, R7679 (2000).
- ⁴ T. Acachi, O. E., K. Kato, H. Kobayashi, T. Miyazaki, M. Tokumoto, and A. Kobayashi, *J. Am. Chem. Soc.* **122**, 3238 (2000).
- ⁵ H. Wilhelm, D. Jaccard, R. Duprat, C. Bourbonnais, D. Jérôme, J. Moser, C. Carcel, and J. M. Fabre, *Eur. Phys. J. B* **21**, 175 (2001).
- ⁶ F. Nad, P. Monceau, C. Carcel, and J. M. Fabre, *Phys. Rev. B* **62**, 1753 (2000).
- ⁷ D. S. Chow, F. Zamborszky, B. Alavi, D. J. Tantillo, A. Baur, c. A. Merlic, and S. E. Brown, *Phys. Rev. Lett.* **85**, 1698 (2000).
- ⁸ D. Jerome, P. Auban-Senzier, L. Balicas, K. Behnia, W. Kang, P. Wzietek, C. Berthier, P. Caretta, M. Horvatic, P. Segransan, et al., *Synth. Met.* **70**, 719 (1995).
- ⁹ L. D. Vescoli, W. H. Henderson, G. Gruner, K. P. Starkey, and L. K. Montgomery, *Science* **281**, 1181 (1998).
- ¹⁰ G. Mihaly, I. Kezsmarki, F. Zamborszky, and L. Forro, *Phys. Rev. Lett* **84**, 2670 (2000).
- ¹¹ H. Seo and H. Fukuyama, *J. Phys. Soc. Japan* **66**, 1249 (1997).
- ¹² S. Mazumdar, R. T. Clay, and D. K. Campbell, *Phys. Rev. B* **62**, 13400 (2000).
- ¹³ R. T. Clay, S. Mazumdar, and D. K. Campbell (2001), cond-mat/0112278.
- ¹⁴ J. P. Pouget and S. Ravy, *J. Phys. I (France)* **6**, 1501 (1996).
- ¹⁵ P. Monceau, F. Y. Nad, and S. Brazovskii, *Phys. Rev. Lett.* **86**, 4080 (2001).
- ¹⁶ S. E. Brown (unpublished).
- ¹⁷ S. E. Brown, W. G. Clark, F. Zamborszky, B. J. Klemme, G. Kriza, B. Alavi, C. Merlic, P. Kuhns, and W. Moulton, *Phys. Rev. Lett.* **80**, 5429 (1998).
- ¹⁸ S. E. Brown, W. G. Clark, B. Alavi, D. S. Chow, C. A. Merlic, and D. J. Tantillo, *Synth. Metals* **103**, 2056 (1999).
- ¹⁹ T. W. Hijmans, H. B. Brom, and L. J. de Jongh, *Phys. Rev. Lett.* **54**, 1714 (1985).
- ²⁰ Y. Fagot-Revurat, M. Horvatic, C. Berthier, P. Segransan, G. Dhalenne, and A. Revcolevschi, *Phys. Rev. Lett.* **77**, 1861 (1996).
- ²¹ V. J. Emery, R. Bruinsma, and S. Barisić, *Phys. Rev. Lett.* **48**, 1039 (1982).
- ²² F. Mila, *Phys. Rev. B* **52**, 4788 (1996).
- ²³ R. Laversanne, C. Coulon, B. Gallois, J. P. Pouget, and R. Moret, *J. Phys. Lett.* **45**, L393 (1984).
- ²⁴ C. Coulon, J. C. Scott, and R. Laversanne, *Phys. Rev. B* **33**, 6235 (1986).